DOI: 10.1002/chem.200501417

Conformational, Concomitant Polymorphs of 4,4-Diphenyl-2,5-cyclohexadienone: Conformation and Lattice Energy Compensation in the Kinetic and Thermodynamic Forms

Saikat Roy,[a] Rahul Banerjee,[a] Ashwini Nangia,*[a] and Gert J. Kruger*[b]

Abstract: 4,4-Diphenyl-2,5-cyclohexadienone (**1**) crystallized as four conformational polymorphs and a record number of 19 crystallographically independent molecules have been characterized by low-temperature X-ray diffraction: form A ($P2_1$, $Z'=1$), form B ($P\bar{1}$, $Z'=4$), form C ($P\bar{1}$, $Z'=12$), and form D ($Pbca$, $Z'=2$). We have now confirmed by variable-temperature powder X-ray diffraction that form A is the thermodynamic polymorph and B is the kinetic form of the enantiotropic system A–D. Differences in the packing of the molecules in these polymorphs result from different acidic C–H donors approaching the C=O acceptor in C–H···O chains and in synthons **I–III**, depending on the molecular conformation. The strength of the C–H···O interaction in a particular structure correlates with the number of symmetry-independent conformations (Z') in that polymorph, that is, a short C–H···O interaction leads to a high Z' value. Molecular conformation (E_{conf}) and lattice energy (U_{latt}) contributions compensate each other in crystal structures A, B, and D resulting in very similar total energies: E_{total} of the stable form A = 1.22 kcal mol^{-1}, the metastable form B = 1.49 kcal mol^{-1}, and form D = 1.98 kcal mol^{-1}. Disappeared polymorph C is postulated as a high-Z', high-energy precursor of kinetic form B. Thermodynamic form A matches with the third lowest energy frame based on the value of U_{latt} determined in the crystal structure prediction (Cerius^2, COMPASS) by full-body minimization. Re-ranking the calculated frames on consideration of both E_{conf} (Spartan 04) and U_{latt} energies gives a perfect match of frame #1 with stable structure A. Diphenylquinone **1** is an experimental benchmark used to validate accurate crystal structure energies of the kinetic and thermodynamic polymorphs separated by <0.3 kcal mol^{-1} (~ 1.3 kJ mol^{-1}).

Keywords: conformation analysis · crystal structure prediction · polymorphism · supramolecular chemistry · symmetry-independent molecule · X-ray diffraction

Introduction

McCrone's[1] definition of a polymorph as "a solid crystalline phase of a given compound resulting from the possibility of at least two different arrangements of the molecules of that compound in the solid state" is widely accepted today.[2] The existence of polymorphism implies that free-energy differences between various forms are small (<3 kcal mol^{-1}) and that kinetic factors are important during crystal nucleation and growth. Molecular conformations, hydrogen bonding, packing arrangements, and lattice energies of the same molecule in different supramolecular environments may be compared in polymorphic structures.[3] Polymorphs are ideal systems to study molecular structure–crystal structure–crystal energy relationships with a minimum number of variables because differences arise due to different intermolecular interactions (supramolecular synthons)[4] and crystal packing effects and not because they are different chemical species. There is increasing interest in understanding polymorphism, growing new crystal forms, controlling the selective growth of one form, transformations between polymorphs, and the high-throughput crystallization of drugs.[5] Polymorphism is more widespread in pharmaceutical

[a] S. Roy, R. Banerjee, Prof. A. Nangia
School of Chemistry, University of Hyderabad
Hyderabad 500 046 (India)
Fax: (+91) 40-2301-1338
E-mail: ashwini_nangia@rediffmail.com

[b] Prof. G. J. Kruger
Department of Chemistry, University of Johannesburg
PO Box 524, Auckland Park, Johannesburg 2006 (South Africa)
Fax: (+27) 11-489-2819
E-mail: gjk@rau.ac.za

Supporting information for this article is available on the WWW under http://www.chemeurj.org/ or from the author. Simulated powder XRD plots of forms A–D, DSC of diphenylquinone **1**, conformational overlay diagram, Rietveld fit of Polymorph Predictor frame with form A, and tables containing crystal structure prediction frames, energies, and cell parameters.

solids[6] than the estimates of 4–5% polymorphic crystals[7] in the Cambridge Structural Database (CSD) suggest.[8] Among organic crystal structures, there is one example of a compound with seven polymorphs (5-methyl-2-[(2-nitrophenyl)amino]-3-thiophenecarbonitrile, common name ROY),[9] sulfathiazole has five forms, there are 14 clusters of tetramorphs, and over a 100 trimorphic systems.[9b,10a] Polymorphism is of great current interest because different solid-state forms can have different physical, chemical, and functional properties, for example, melting point, stability, color, bioavailability, pharmacological activity, and a nonlinear optical response.

Concomitant polymorphs[11] crystallize simultaneously from the same solvent and crystallization flask under identical crystal growth conditions. Bernstein[12] carried out early studies on conformational polymorphs (different conformations of the same molecule in different crystal structures) and conformational isomorphs (different conformers of the same molecule in the same crystal structure). Herein we describe a tetramorphic cluster of conformational polymorphs in which molecular- and lattice-energy compensation results in very small differences in the total energy of the concomitant polymorphs A–D of 4,4-diphenyl-2,5-cyclohexadienone (**1**). Experimental conditions are described for the preparation of thermodynamic form A and kinetic form B in a reasonably pure state. The implication of a molecular and crystal-packing balance is to rank crystal structure prediction frames derived from metastable rotamers by consideration of both conformation- and lattice-energy contributions, which gives an excellent match of the global minimum structure with stable form A.

Results and Discussion

Crystal packing and multiple Z' in polymorphs: Crystallographic data for the polymorphs A–D of diphenylbenzoquinone **1** are listed in Table 1.[13] The molecule has several acidic, activated donor hydrogen atoms of sp^2- and phenyl C–H-type whereas there is a single carbonyl acceptor. Depending on the molecular conformation one or more of the several possible C–H···O interactions[14] are optimized in the crystal structure (Figure 1). For example, form A has zigzag chains of C–H···O interactions between screw-axis-related A_i molecules of graph-set notation[15] $C(8)$. Form B has C–H···O quinone dimer synthon **I** and *p*-phenyl C–H···O synthon **II** [graph set $R_2^2(8)$ and $R_2^2(20)$] between B_i, B_{ii} and B_{iii}, B_{iv} molecules, respectively. Form C has the same synthons and overall packing as B but has 12 molecules (C_i–C_{xii}) in the asymmetric unit. Form D has $C(10)$ chains that connect to form the cyclic $R_4^3(32)$ pattern and *o*-phenyl C–H···O synthon **III** with a

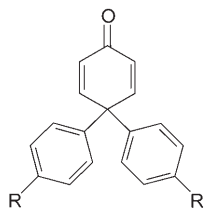

1: R = H
2: R = Ph
3: R = Cl, Br, Me

Table 1. Crystallographic data for polymorphs A–D of diphenylquinone **1**.[13]

	Form A	Form B	Form C	Form D
CSD refcode[a]	HEYHUO	HEYHUO01	HEYHUO02	HEYHUO03
space group	$P2_1$	$P\bar{1}$	$P\bar{1}$	*Pbca*
Z', Z	1, 2	4, 8	12, 24	2, 16
a [Å]	7.9170(6)	10.0939(2)	18.3788(4)	10.7921(6)
b [Å]	8.4455(6)	16.2592(3)	19.9701(4)	17.4749(12)
c [Å]	10.3086(9)	16.2921(4)	24.4423(5)	27.9344(19)
α [°]	90	88.2570(10)	95.008(1)	90
β [°]	105.758(2)	85.3380(10)	111.688(1)	90
γ [°]	90	83.6450(10)	105.218(1)	90
V [Å^3]	663.36(9)	2648.00(10)	7871.8(3)	5268.2(6)
R factor	0.050	0.068	0.112	0.059

[a] See ref. [8].

$R_2^2(16)$ ring through D_i and D_{ii} molecules. The parameters of the C–H···O geometries are listed in the legend to Figure 1. We have not found polymorphs of bis(biphenylyl) ketone **2**[16] or its substituted phenyl derivatives **3** (4-Cl/Br/Me)[10b] so far.

The number of symmetry-independent or crystallographically unique molecules/ions in a crystal lattice is Z'. Alternatively, Z' may be defined as the number of formula units (Z) divided by the number of independent general positions for that space group. Z' is typically 1 or 0.5 in crystal structures (87%). A high Z' of 12 for form C is a record for polymorph clusters[9b] (Table 2) and as such rare in the CSD[8] (only five hits).

Structures with high Z' values continue to interest crystallographers but it is still not properly understood why some categories of structures exhibit a higher frequency of $Z'>1$. Steed[17] has critically reviewed the reasons for high-Z' crystal structures. 1) The molecule has a packing problem because of its awkward shape, which is reconciled by having two or more molecules in different conformations.[18] 2) The molecules organize in stable clusters prior to reaching the highest symmetry arrangement in strong O–H···O hydrogen-bonded structures because of the enthalpic advantage derived from σ-cooperative chains,[19] for example, as in alcohols, phenols, steroids, nucleotides, and nucleosides. 3) Several low-lying molecular conformations interconvert in solution and more than one molecule may crystallize simultaneously for kinetic reasons. The last of these situations occurs in the conformational polymorphs of **1**, which provides a unique opportunity to study polymorphic structures with multiple values of Z'.

Cholesterol ($Z'=16$) is a prototype example of strong O–H···O hydrogen bonds being associated with unusually high Z' values. An exceptional case in the weak hydrogen bond category is the crystal structure $[ReCl_2(NCMe)(NO)(PMe_3)_2]$ (CSD refcode WODCOH, $Z'=11$),[20] which has a dense network of C–H···O and C–H···Cl interactions. We observed an interesting trend in the polymorphs of **1**, namely that the number of conformations in a particular structure (Z') correlates with C–H···O bond strength/distance. Figure 2 is a distance–angle scatter plot of C–H···O interactions in polymorphic forms A–D. C–H···O contacts in form C are, in general, shorter than those in forms B and D

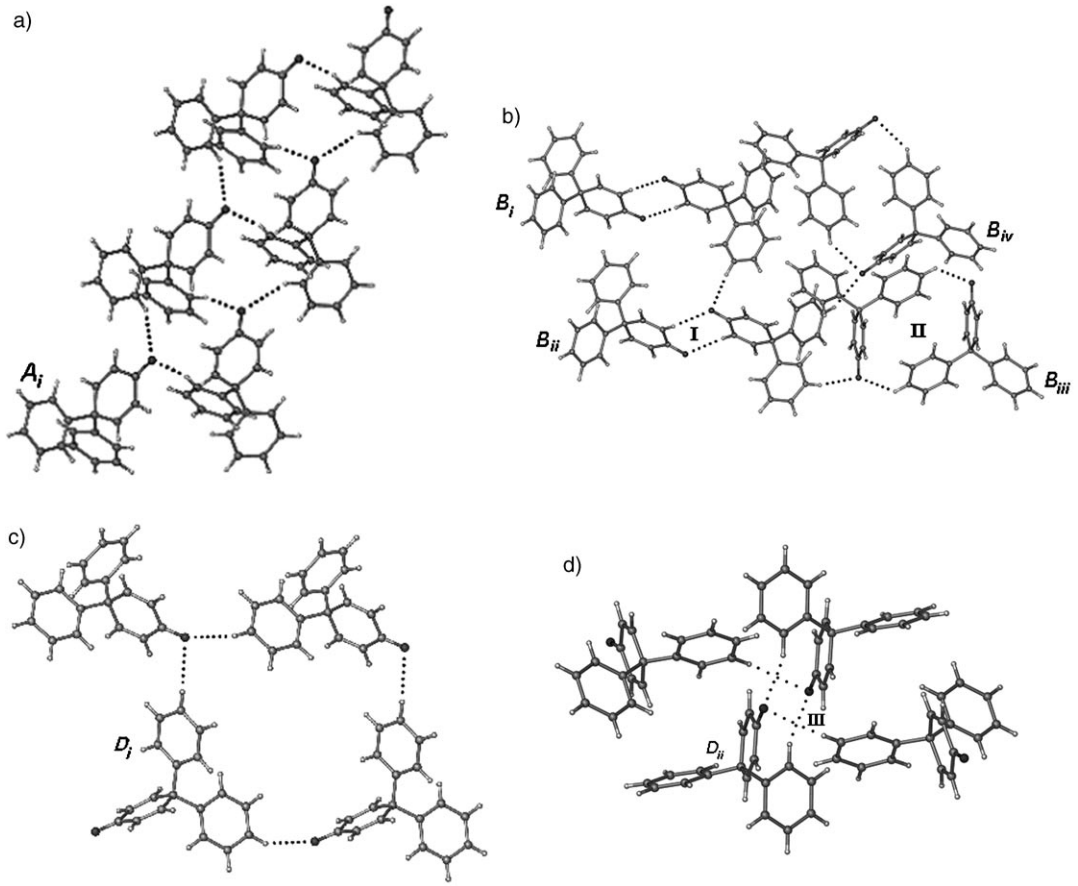

Figure 1. a) Helices of C–H···O hydrogen bonds (2.55 Å, 163.6°; 2.60 Å, 129.9°) between 2_1 related molecules in form **A** [conformer A_i, graph set $C(8)$]. b) Centrosymmetric C–H···O synthon **I** between B_i, B_{ii} molecules of $R_2^2(8)$ pattern (2.33 Å, 169.2°; 2.49 Å, 123.5°) and synthon **II** between B_{iii}, B_{iv} molecules of $R_2^2(20)$ pattern (2.64 Å, 138.0°; 2.74 Å, 121.6°) in form **B**. The crystal structure of form **C** is similar to **B**. Twelve symmetry independent molecules (C_i–C_{xii}) engage in similar synthons instead of four molecules in B. c) C–H···O interactions of graph set $R_4^3(32)$ between translation and screw-axis-related D_i molecules (2.36 Å, 137.9°; 2.54 Å, 166.9°) in form **D**. d) Centrosymmetric C–H···O synthon **III** between D_{ii} molecules [$R_2^2(16)$ pattern] and C–H···O interaction (2.57 Å, 144.5°; 2.47 Å, 165.1°). Neutron-normalized distances are quoted. Note that different C–H donors participate in C–H···O interactions in different crystal forms. Cyclic C–H···O synthons **I–III** are labeled.

Table 2. Data for polymorphs ($\geq$3 forms)[a] in organic crystal structures with multiple molecules in the asymmetric unit.

Entry	CSD refcode[b]	No. of polymorphs	Highest Z′
	conformational polymorphs ($\geq$4 forms)[a]		
1	QAXMEH	7	1
2	SUTHAZ	5	2
3	BEWKUJ	4	2
4	BIXGIY	4	1
5	HEYHUO[c]	4	12
6	KAXHAS	4	1
7	MABZNA	4	4
8	RUWYIR	4	2
	multiple molecules in asymmetric unit ($Z'>4$)[a]		
9	PUBMUU[c]	3	16
10	IFULUQ	4	8
11	DUVZOJ	3	6
12	ZZZVTY	3	5
13	THIOUR	3	4.5

[a] Cut-offs were made to limit the number of structures analyzed. [b] See ref. [8]. [c] Compound has a high number of polymorphs and a high Z' value.

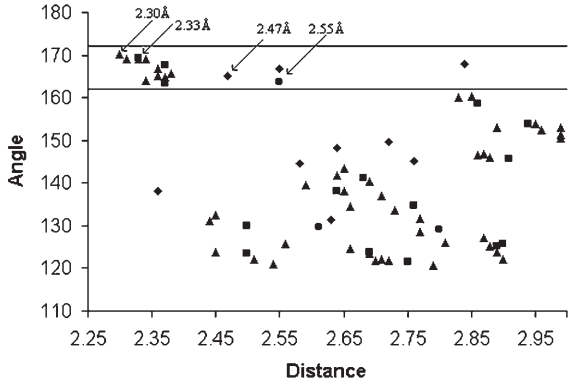

Figure 2. H···O distance (2.2–3.0 Å) versus C–H···O angle (120–180°) scatter plot of interactions in tetramorphs A–D. A = ● ($Z'=1$), B = ■ ($Z'=4$), C = ▲ ($Z'=12$), D = ◆ ($Z'=2$). The shortest H···O distance (marked with an arrow in the linear band) is inversely related to Z' (the number of symmetry-independent conformations).

and longer in form A. Interestingly, the shortest linear interaction ($\theta = 160$–$175°$) in a particular form is inversely related to the Z' value of that structure: for example, form C has the shortest H···O distance of 2.30 Å and the highest Z' value of 12, form B has H···O = 2.33 Å, $Z' = 4$, and forms D and A have even longer H···O distances of 2.47 and 2.55 Å and smaller Z' values of 2 and 1, respectively. Our finding that the strength of C–H···O interactions can promote $Z' > 1$ among flexible molecules means that the well-known examples of structures with values of $Z' > 1$, that is, alcohols and phenols, can be expanded to new categories of crystal structures stabilized by weak hydrogen bonds. We show that the relative strengths of directional C–H···O interactions are important in promoting high Z' structures[21] particularly as their energies are comparable to favorable close-packing forces. The inverse relationship between Z' and H···O distance is observable in polymorphic cluster **1** because detailed supramolecular effects can be clearly discerned against a background of a constant molecular structure.

The occurrence of high-Z' polymorphs and the relationship between Z' and C–H···O strength alludes to the importance of kinetic factors during crystallization. We therefore wanted to identify which of the concomitant polymorphs A–D is the kinetic form and which is the thermodynamic one and determine the nature of the phase transitions between these forms.

Variable-temperature powder X-ray diffraction: We obtained single crystals of all four forms in preliminary batches[13] but subsequent experiments gave mostly forms A and B, as determined by unit-cell checking of several crystals. However, powder X-ray diffraction shows all four forms in the concomitant mixture at room temperature (Figure 3). A typical solid upon crystallization from EtOAc/*n*-hexane contains form A (~40%), forms B+C (~50%), and form D (~10%). The ratios were determined by the Rietveld refinement[22] of observed powder XRD plots with simulated peaks for each crystal structure (Powder Cell 2.3). Triclinic forms B and C are taken together because it is not possible to distinguish between these closely related forms from their overlapping diffraction patterns (Figure S1, Supporting information). The mixture of forms at room temperature was heated to study phase transformations. The peak profile is relatively stable between 30–60 °C, however, we noticed changes as the sample was heated to 70 °C (Figure 4): Certain peaks disappeared and the overall pattern became significantly sharper with fewer but more intense lines. The PXRD profile is relatively unchanged between 70–100 °C, after which the material became mostly amorphous and then gradually turned to a semi-solid/melt mass at 105–115 °C. There are no reflections from the sample at $T >$ 105 °C except for the peak from the sample holder at 25.2°. VT-PXRD shows that heating polymorphs A–D to a pre-melt temperature of 70 °C transforms the mixture to form A (Figure 5) with good polymorph purity (> 95%), based on a match with simulated peaks of the crystal structure. Monoclinic polymorph A therefore is a thermodynamic modification of the enantiotropic system of polymorphs **1** between 30–80 °C.

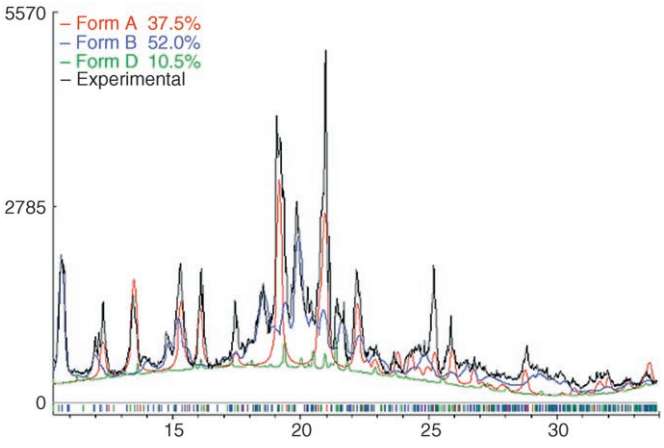

Figure 3. Powder X-ray diffraction of solid **1** at room temperature: black = experimentally observed powder pattern; red, blue, and green = calculated powder pattern of form A (37.5%), B+C (52.0%), and D (10.5%), respectively. Rietveld refinement in Powder Cell 2.3: $R_p = 14.82$, $R_{wp} = 19.32$. Percentages of polymorphic forms in different batches vary within 5%.

Chiral form A was prepared in high purity and shown to have a nonlinear optical signal equal to that of urea when irradiated with a Nd^{3+}–YAG laser (1.06 μm). However, the mixture of polymorphs obtained from a typical solution crystallization does not emit light at 532 nm. The preparation of form A by the above heating method is preferred over controlled crystallization at −5 °C because of contamination from other polymorphs over a period of time, presumably due to accidental seeding of laboratory space,[23] a term used to describe difficulties in isolating an early polymorph after the appearance of other forms of the same compound. Polymorphs of **1** do not follow Ostwald's rule of stages,[24] with stable form A appearing first from solution crystallization followed by metastable forms B and C.

Kinetic form B was prepared by heating the polymorphic mixture to a melt phase in the powder X-ray diffractometer pan at ~115 °C. Cooling the sample to room temperature afforded reasonably pure polymorph B (Figure 6). This was confirmed by unit-cell checking of a few randomly picked crystals. Although polymorphs A–D have quite different arrangements of molecules and unit cells, they melt at the same temperature ($T_m = 120.45$ °C) and there is no apparent phase transition other than the melting endotherm in differential scanning calorimetry (Figure S2, Supporting information).

There are alternative explanations for the occurrence of concomitant polymorphs:[11] Simultaneous nucleation of more than one form from solution, interconversion between polymorphs, their appearance in order of stability, and heterogeneous cross nucleation.[5e] The simultaneous crystallization of all four forms A–D from the homogeneous medium is the most likely reason for the concomitant cluster **1**. Interconversion in solution is minimal at room temperature be-

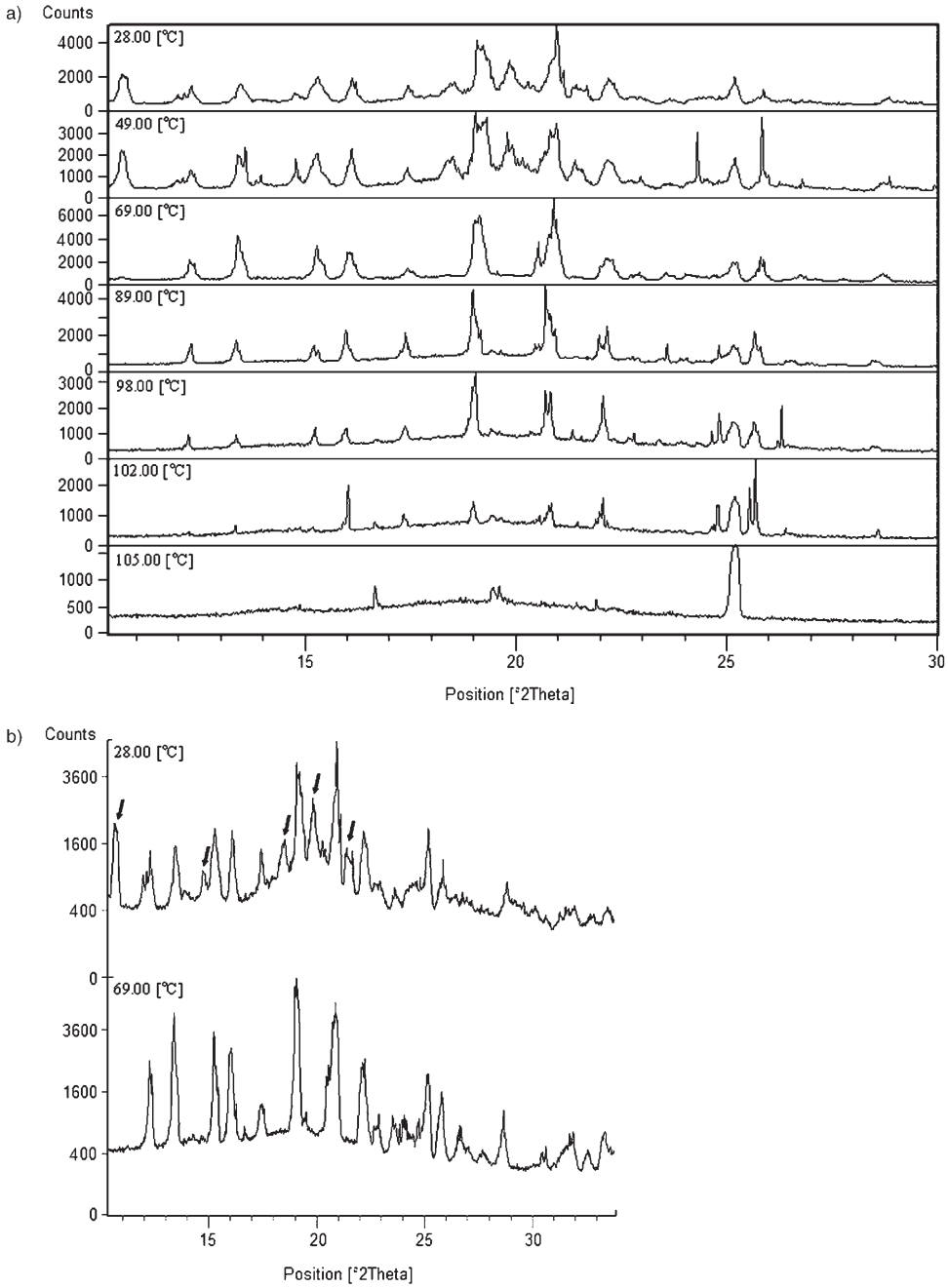

Figure 4. a) Powder X-ray diffraction patterns of **1** recorded at different temperatures. The sample is a mixture of forms A–D at room temperature, it transforms to forms A at around 70 °C, and becomes amorphous upon further heating to 105 °C. The wide peak at 25.2° is from the sample holder. b) Powder XRD of **1** at 28 (top) and 69 °C (bottom). Peaks that disappear upon heating are marked with an arrow. Note the increase in intensity of the peaks and the overall simplification of the profile at a higher temperature.

cause the percentages of various forms in different batches are within the experimental limit of 5%. As mentioned, the system does not obey Ostwald's law of stages. Heterogeneous cross nucleation in the heated/melt phase is ruled out because if this were happening then cooling the sample from 70 and 115 °C would not only give form A and B, respectively, but also other polymorphs from seeded nucleation and growth.

Conformation and lattice energy compensation: Compound **1** is an excellent system for studying how interconverting molecular conformations in solution lead to different crystal packing arrangements involving several conformers in the solid state. The energies of the molecular conformations and the crystal lattice were calculated to obtain a quantitative picture of polymorphism in **1** and a clue as to why these conformational polymorphs appear concomitantly. The conformation energies (E_{conf}) and dipole moments (μ) were calculated using the Spartan 04 package[25] (Table 3). Each molecule was extracted from the crystal structure and energy-minimized (HF/6-31G**) keeping the conformation fixed (heavy carbon and oxygen atoms invariant) while the hydrogen atoms were allowed to relax to reasonable geometries following the method of Yu et al.[9a] The torsion angles τ_1 and τ_2 that define the rotation about the $C_{quinone}$–C_{phenyl} single bonds lie in the range of 8–22 and 12–38°, respectively, along the scatter plot diagonal (Figure 7). In general, in the 19 rotamers $\tau_1 \neq \tau_2$ save conformer A_i and C_{xi} (see Figure S3, Supporting information, for the overlay diagram). Molecule B_i has the most stable conformation ($E_{conf} = -479\,813.50$ kcal mol^{-1}, a value that is arbitrarily fixed to 0); the energies of the conformers of forms A, B, and D (E_{conf}) are within 1.3 kcal mol^{-1} of B_i (Table 3). Conformers C_i–C_{xii} are higher in energy ($E_{conf} = 2$–9 kcal mol^{-1}) but this could be due to an error in the experimental X-ray geometry as the *R* factor of form C is high (11.1%). Therefore we focus on structures A, B, and D in this discussion. The conformers of forms A, B, and D readily interconvert in solution through geared (correlated) rotation of the phenyl rings[13] about τ_1 and τ_2 because the energy barrier should be accessible through the thermal motion of atoms ($RT \sim 0.5$ kcal mol^{-1} at 298 K) in the crystallization regime between −5 and 100 °C.

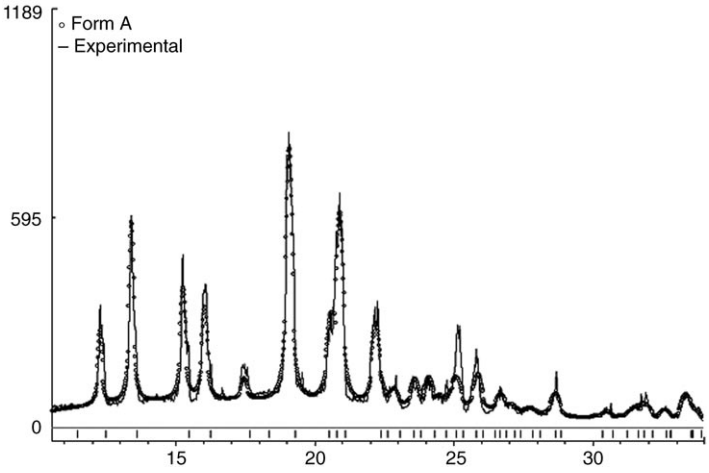

Figure 5. Experimental powder XRD of **1** at 69 °C (black line) matches with the calculated powder pattern of polymorph A (dotted line). Rietveld refinement in powder cell 2.3: $R_p = 14.39$, $R_{wp} = 18.81$. The starting solid was the mixture of forms A–D shown in Figure 3.

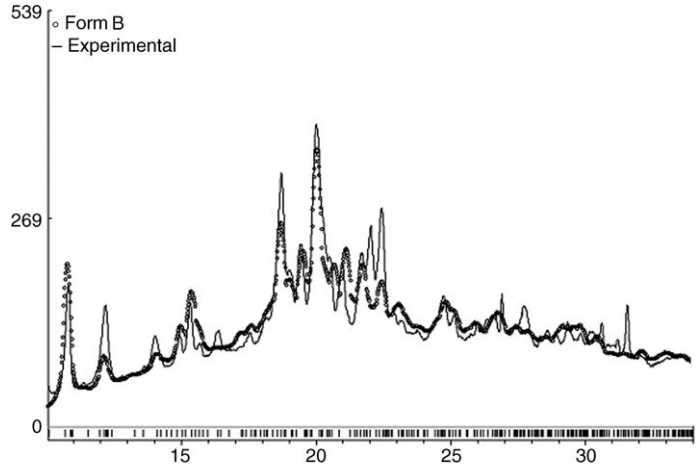

Figure 6. Experimental powder XRD of **1** from melt crystallization at 115 °C (black line) shows good agreement with the calculated powder pattern of polymorph B (dotted line). Rietveld refinement in powder cell 2.3: $R_p = 11.78$, $R_{wp} = 15.86$. The starting solid was the mixture of forms A–D shown in Figure 3.

The crystal lattice energies, U_{latt}, of polymorphs A–D were computed using the COMPASS and DREIDING 2.21 force fields (Table 4, Cerius^2).[26] We discuss COMPASS numbers because this force field is better parametrized and gives more accurate energies of organic molecules[27] that are typically stabilized by hydrogen bonds, intermolecular interactions, and van der Waals forces. COMPASS[28] is better suited for molecule **1** because electrostatic stabilization by C–H···O hydrogen bonds and edge-to-face aromatic interactions is included in the coulombic term. Form A has the most stable crystal structure ($U_{latt} = -32.69$ kcal mol^{-1}) and forms B, C, and D are less stable by 1.03, 1.06, and 0.82 kcal mol^{-1}, respectively. However, all these crystal structures are a compromise between intra- and intermolecular stability. Either the molecular conformer or the lattice energy is at the minimum, but both intra- and intermolecular energies are not the lowest in any structure. For example, form A has the lowest U_{latt} value (-32.69 kcal mol^{-1}), but conformer A_i is higher in energy ($E_{conf} = 1.22$ kcal mol^{-1}). Molecular conformations B_i–B_{iv} are lower in energy ($E_{conf} =$ 0.00, 0.06, 0.66, 1.12 kcal mol^{-1}) but crystal lattice B is metastable ($U_{latt} = -31.66$ kcal mol^{-1}). Both intra- and intermolecular energy contributions are included in the total energy term (Table 5). In increasing order of E_{total} (COMPASS): form A (thermodynamic, most stable) < B (kinetic, intermediate stable) < D (least stable). This energy order is consistent with the thermodynamic stability of form A determined in the VT-PXRD experiments and the crystallization of the kinetic form B from the melt of the polymorphic mixture. On the other hand, the U_{latt} (COMPASS) stability order of A < D < B and the energies calculated by using the DREIDING 2.21 force field (D < A < B) do not agree with experiment. We believe that calculations using the COMPASS force field give an indication of the relative stability of the polymorphs with an energy difference of 0.3–1.0 kcal mol^{-1} for small organic molecules.

The molecular conformations and crystal lattice energies suggest the following picture of polymorphism in **1**. Depending on the geometry of a particular conformation, a different C–H···O interaction and aromatic packing motif lead to a metastable crystal structure. The reason for conformational polymorphism in **1** is that C–H···O motifs in its crystal structures (Figure 1) involve one of the phenyl C–H donors, except for those in dimer **I** which are between the quinone groups. Therefore a change in molecular conformation will alter the strength of weak C–H···O and van der Waals interactions and in turn the preferred crystal-packing motif. The energy penalty in the molecular conformation is compensated by lattice-energy gain from intermolecular interactions and close packing, and vice versa, because their magnitudes are comparable, $\Delta E_{conf} \approx \Delta U_{latt} = 0$–2 kcal mol^{-1}. Facile rotamer interconversion in solution and very similar crystal energies mean that more than one molecular conformation may crystallize out simultaneously to give concomitant conformational polymorphs of **1**.

Price and co-workers[29] recently examined intra- and intermolecular energy compensation in the conformational polymorphs of some drugs, for example, aspirin, barbituric acid, and piracetam. Surprisingly, the quintessential polymorphic compound, ROY, appears to be an exception to the above-mentioned energy balance situation: the stable perpendicular conformation is present in the thermodynamic yellow crystal form.[30] This prompts the question: Will metastable crystal forms of ROY give way to the stable polymorph because the system may gradually transform to the bottom of the molecular and lattice energy well?

Having discussed forms A, B, and D we will briefly mention the unusually high Z' value (= 12) of polymorph C. We previously postulated[13] that form C represents a snap-shot picture of an evolving crystal nucleus on the way to form B ($Z' = 4$) wherein the molecules have aggregated to form the

Table 3. Energies and dipole moments of 19 conformers of **1** calculated using Spartan 04.

Crystal polymorph	Molecular conformation[a]	Ph torsion angles		HF/6-31G**	
		τ_1 [°]	τ_2 [°]	E_{conf}[b] [kcal mol^{-1}]	μ [D]
form A	A_i	12.5	12.6	1.22	5.15
form B	B_i	12.3	16.0	0.00	5.22
	B_{ii}	14.9	23.6	0.06	5.20
	B_{iii}	19.1	31.8	0.66	5.34
	B_{iv}	11.5	17.7	1.12	5.24
form C	Ci	12.8	16.0	2.81	5.20
	C_{ii}	11.9	16.7	3.94	5.40
	C_{iii}	18.4	32.3	4.16	5.06
	C_{iv}	12.1	22.7	4.76	5.30
	C_v	15.2	22.0	5.19	5.40
	C_{vi}	10.2	21.0	5.51	5.24
	C_{vii}	11.5	17.4	7.99	5.50
	C_{viii}	18.3	28.2	8.14	5.08
	C_{ix}	20.9	30.8	8.15	5.21
	C_x	14.0	16.7	8.31	5.15
	C_{xi}	14.9	15.1	8.54	5.23
	C_{xii}	20.1	31.5	8.90	5.39
form D	D_i	18.5	36.8	1.08	5.21
	D_{ii}	8.4	16.5	1.25	5.17
energy-minimized[c]		22.3	22.3	−2.78	4.87

[a] Molecules are numbered in order of increasing energy. [b] Conformer B_i has the most stable conformation (−479813.50 kcal mol^{-1}) and is arbitrarily fixed to 0.00 for comparison of conformation energies. [c] The molecular skeleton was minimized to the stable gas-phase rotamer.

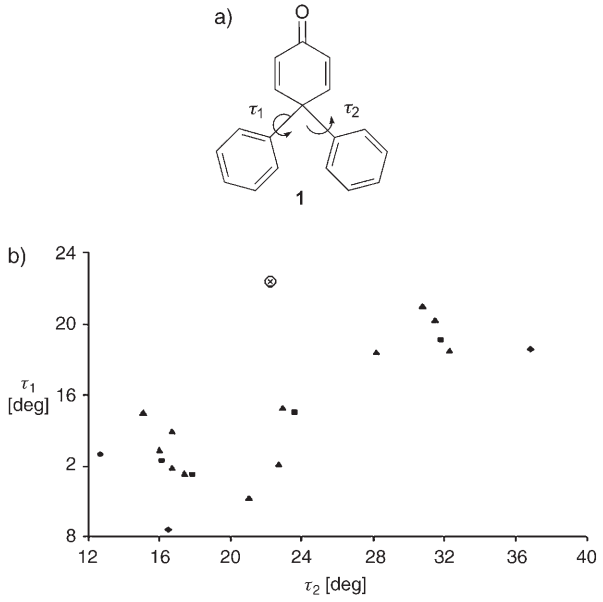

Figure 7. a) Conformations of diphenylquinone **1** defined by torsion angles τ_1 and τ_2 about the $C_{quinone}$–C_{phenyl} single bonds. b) Nineteen crystallographically independent conformations of **1** lie along the diagonal. All 19 conformers converge to the gas-phase rotamer ($\tau_1=\tau_2=22.3°$) after energy minimization. A = ●, B = ■, C = ▲, D = ◆, and gas phase = ⊗.

crystal lattice but the periodicity is yet to reach the highest possible crystal symmetry. The 12 high-energy conformers of crystal structure C may be viewed as metastable relics of the relatively stable four conformers of form B. Attempts to study the transformation of form C to B in the laboratory were thwarted by our inability to grow crystals of form C after the initial X-ray diffraction experiment. The above interpretation is consistent with the following observations. 1) The higher-energy conformers in form C participate in stronger C–H···O interactions and this alludes to the greater role of kinetic factors in the nucleation of this polymorph. 2) The close relationship between forms C and B is evident from their crystal structures: They have the same space group and overall packing that is sustained through C–H···O synthons **I** and **II** and overlapping powder XRD peaks. In short, high Z' structures are not just a crystallographic oddity but they open a window to "see" crystal nucleation and growth.

Does molecular conformation determine crystal packing or are favorable crystal packing effects able to trap metastable molecular conformations? This question is difficult to quantify in the present case because E_{conf} and U_{latt} differences are of the same order of magnitude. We can nonetheless say that a particular conformation is associated with a specific C–H···O synthon even though that rotamer is present in different polymorphs. For example, B_{iv} and C_{vii} rotamers have similar conformations and they engage in synthon **II** in the crystal structures of polymorphs B and C. Such a reality, namely that a less stable conformation can lead to a more stable crystal lattice in conformational polymorphs, is a major challenge in the crystal structure prediction of flexible molecules.

Computational prediction of form A: The ab initio prediction of crystal structures of organic molecules from their molecular diagram is a global research activity,[31] which should give us a better understanding of the crystallization process and even protein folding. In crystal structure prediction (CSP), the input for flexible molecules is progressing from the first phase of using stable gas-phase conformations to metastable conformations.[29] The main difficulties in predicting the structures of conformationally flexible molecules are the following. 1) The stable conformation may not result in the thermodynamic crystal structure. 2) Which metastable conformation out of several low-energy rotamers should be selected for simulations? 3) Both conformation- and lattice-energy contributions to crystal structure stabilization must be taken into account. These issues are pertinent to molecule **1** and we now present a possible solution for predicting and ranking structure frames of a conformationally flexible molecule. Thermodynamic polymorph A is the target in crystal structure prediction because at the present time CSP computations are only able to predict the lowest energy

Table 4. Lattice energies [U_{latt}, kcal mol^{-1}] of forms A–D computed in Cerius^2, corrected to per molecule of **1**.

	Form A		Form B		Form C		Form D	
U_{latt}	COMPASS	DREIDING 2.21	COMPASS	DREIDING 2.21	COMPASS	DREIDING 2.21	COMPASS	DREIDING 2.21
total	−32.69	−42.12	−31.66	−39.66	−31.63	−39.71	−31.87	−42.42
van der Waals	−28.01	−27.78	−28.19	−27.22	−28.18	−27.23	−27.80	−27.19
coulombic	−4.68	−12.50	−3.47	−10.43	−3.45	−10.49	−4.07	−12.49
hydrogen bond[a]	–	−1.84	–	−2.01	–	−1.99	–	−2.74

[a] The hydrogen bond energy is partitioned in the DREIDING 2.21 force field but it is part of the coulombic component in the COMPASS force field.

Table 5. Relative energies[a] [per molecule, kcal mol^{-1}] of crystal forms A, B, and D.[b]

Polymorph	U_{latt}		E_{conf}[c]	$E_{total} = U_{latt} + E_{conf}$		Graph set symbol of C–H···O interaction
	COMPASS	DREIDING 2.21	HF/6-31G**	COMPASS	DREIDING 2.21	
A	0.00	0.30	1.22	1.22	1.52	$C(8)$
B	1.03	2.76	0.46	1.49	3.22	$R_2^2(8)$, $R_2^2(20)$
D	0.82	0.00	1.16	1.98	1.16	$R_2^2(16)$, $R_4^3(32)$

[a] Values taken from Tables 3 and 4. The values of U_{latt} and E_{conf} are relative energies. [b] Form C is excluded because the errors are too large. [c] The average E_{conf} value is estimated for multiple conformers as $(\Sigma E_{conf})/Z'$.

structure and those with $Z' = 1$. The objective of our simulations was to reproduce the known stable polymorph A and to identify structures of similar energies as a guide for future crystallization experiments. We have used Polymorph Predictor (Cerius^2)[26] (PP) computations to generate several putative crystal structures of **1** from the stable molecular conformation derived from Gaussian 03.[32]

In structure prediction, the conformation should be allowed to vary during the energy minimization of frames (defined as full-body minimization) to cover the complete range of possible crystal structures in flexible molecules. Rigid-body minimization (the molecular conformation is held fixed) is about five times faster but it generates structures that correspond to local minima for a particular conformation, not necessarily the global minimum. Crystal structure frames were generated in six common space groups, $P2_1/c$, $P\bar{1}$, $C2/c$, $Pbca$, $P2_1$, and $P2_12_12_1$. Ten unique low-energy frames within 4 kcal mol^{-1} of the global minimum are plotted for each space group in Figure 8 (total of 60 structures, see Table S1, Supporting Information, for values). The experimental structure A is the third rank frame based on values of U_{latt}. Cell parameters, torsion angles, and the lattice energy of CSP frame #3 match remarkably well the experimental structure A having a deviation of within 3% (Table 6). The crystal packing in the simulated structure is identical to the observed form and their powder XRD profiles are in good agreement (Figure 9 and Figure S4, Supporting Information). Although the fact that frame #3 matches the observed structure is short of the correct answer, our reproduction of a large and flexible molecule (compound **1**) is quite good in relation to ongoing CSP efforts by other groups.[31]

How important is the starting conformation in generating a particular crystal structure of **1**? Given that the molecular conformation, C–H···O synthon and crystal packing are inti-

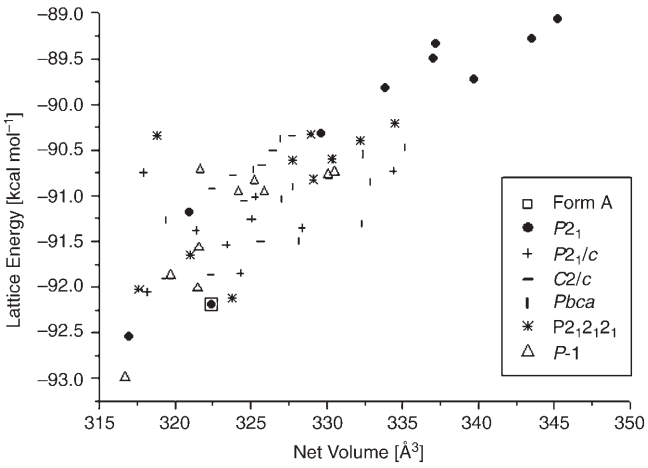

Figure 8. Lattice energy versus net volume (V/Z) for structures of molecule **1** generated in six common space groups by full-body minimization using the Polymorph Predictor software package. Experimental crystal structure A matches with the third rank predicted structure based on values of U_{latt}. See Table 6 for details.

Table 6. Comparison of predicted[a] and experimental[b] structure parameters.

Form	a [Å]	b [Å]	c [Å]	β [°]	V/Z [Å^3]	τ_1, τ_2 [°]	U_{latt} [kcal mol^{-1}]
full-body minimization							
frame #3	7.712	8.286	10.415	104.32	322.45	14.6, 15.9	−92.201
form A	7.713	8.286	10.415	104.32	322.46	14.6, 15.9	−92.196
rigid-body minimization							
frame #1	7.699	8.133	10.165	104.96	307.51	12.6, 12.7	−32.697
form A	7.701	8.139	10.160	105.00	307.54	12.6, 12.7	−32.695
crystallographic parameters from Table 1[c]							
form A	7.917	8.445	10.308	105.75	331.68	12.5, 12.6	–

[a] Structure predicted by Cerius^2 (COMPASS). [b] Experimental form A minimized in Cerius^2. [c] The deviation in cell parameters from those of the full-body minimized structure #3 is <3%.

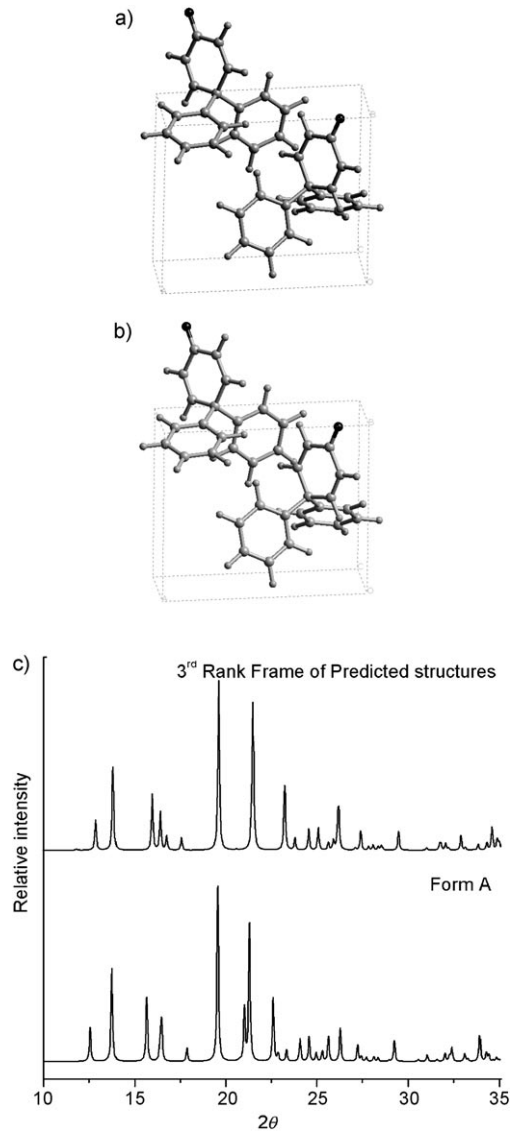

Figure 9. Comparison of experimental stable polymorph A with simulated structure #3 derived from full-body minimization. a) Unit-cell packing in predicted frame #3. b) Unit-cell packing in form A. c) Simulated powder XRD of predicted and experimental crystal structures. See Figure S4, Supporting Information, for Rietveld refinement of PXRD.

mately related in the polymorphs of **1**, we were encouraged to find that rigid-body minimization starting from rotamer A_i gave the lowest energy structure #1 as polymorph A (Table 6). To further attest the significance of metastable conformations in generating structures of **1**, the gas-phase conformation, which is not observed in any known polymorph so far, was used in CSP. Predicted structures from the stable Gaussian 03 rotamer ($\tau_1=\tau_2=23.8°$) are less stable ($U_{latt}=-28$ to $-30\,kcal\,mol^{-1}$, Table S2, Supporting Information) than the observed crystal structures ($U_{latt}=-31$ to $-33\,kcal\,mol^{-1}$, Table 4) with metastable conformations.

The discussions so far imply that the contribution of molecular conformation energy to crystal structure stabilization is significant and so one should accurately compute both intramolecular and intermolecular energy terms. Structures predicted by full-body minimization adopt the best molecular conformation for a stable crystal structure in that space group because the conformation is allowed to adjust during the simulation. The lattice energy quantifies the intermolecular component arising from hydrogen bonds, electrostatic interactions, and van der Waals forces. The gain/penalty from the molecular conformation must be added/subtracted to accurately calculate the total crystal energy. To implement this method, the U_{latt} component was calculated by rigid-body minimization[33] and E_{conf} was calculated using Spartan 04. The starting rotamer was extracted from the full-body minimization frame and structures were generated by the rigid-body method. The minimum energy structure in the rigid-body simulation matches with the full-body reference frame in all respects: Cell parameters, crystal packing, and simulated PXRD (Table S3, Supporting Information). Frame numbers 1–10 of the flexible-body method (Table S1) were re-ranked based on the total energy, $E_{total}=E_{conf}+U_{latt}$, of rigid-body minimized frames (Table 7). There is significant reorganization in the rankings of predicted structures when accurately calculated crystal lattice and molecular conformation energies are considered together to prioritize the simulated frames using increasing E_{total} as the criterion instead of only U_{latt}. Frame #3 of the flexible-body minimization is now the global minimum frame #1 and it perfectly matches stable form A. We take advantage of both the flexible-body and rigid-body minimization methods in Cerius^2 Polymorph Predictor to simulate the crystal structures of a molecule with several low-energy conformations. The best metastable conformation for generating stable crystal packing is determined by allowing torsion angles to vary. Then U_{latt} and E_{conf} are accurately calculated for this ideal conformation and their sum is taken to finalize the lowest energy structure. The above iterative method for deriving the correct metastable conformation and then re-ranking predicted crystal structure frames is not reported in the CSP literature to our knowledge. It is suitable for structure prediction of flexible drug molecules in which conformation- and lattice-energy contributions must be properly quantified.

Among the 60 predicted structures (Table S1, Supporting Information), the molecular conformation in global minimum frame #1 in the $P\bar{1}$ space group (τ_1, $\tau_2=28.4$, 28.6°, $E_{conf}=2.55\,kcal\,mol^{-1}$) is not too high in energy relative to the stable rotamer B_i and may be accessible if a much more stable U_{latt} is able to compensate for the E_{conf} penalty through stronger intermolecular interactions and better close packing. We are searching for new polymorphs of **1** through exhaustive crystallization screens.[34]

Conclusion

Our experimental and computational results on tetramorphic cluster A–D of diphenylquinone **1** can be summarized as follows. 1) Variable-temperature powder XRD shows that

Table 7. U_{latt} of the lowest energy frame determined by the rigid-body method starting from the molecular conformation in full-body minimized frames #1–10. E_{conf} is calculated in Spartan 04. The simulated structures of **1** are re-ranked based on the sum of the intra- and intermolecular energies, E_{total} [kcal mol^{-1}].

Frame # in full-body method[a]	Space group[b]	U_{latt} in rigid-body method [kcal mol^{-1}]	E_{conf}[c] [kcal mol^{-1}]	$E_{total} = U_{latt} + E_{conf}$ [kcal mol^{-1}]	Re-ranked frame based on E_{total}
3	$P2_1$[d]	−30.93	1.38	−29.55	1
1	$P\bar{1}$	−30.83	2.03	−28.80	2
6	$P2_12_12_1$	−30.91	2.25	−28.66	3
10	$C2/c$	−30.42	1.82	−28.60	4
7	$P\bar{1}$	−30.88	2.59	−28.29	5
8	$C2/c$	−30.06	1.82	−28.24	6
5	$P2_1/c$	−30.85	2.79	−28.06	7
4	$P2_12_12_1$	−30.01	2.14	−27.87	8
2	$P2_1$	−31.03	3.27	−27.76	9
9	$P\bar{1}$	−29.88	2.37	−27.51	10

[a] Taken from Table S1. [b] See Table S3 for matching cell parameters. [c] Relative to the stable gas-phase rotamer, $E_{conf} = -479\,812.98$ kcal mol^{-1}. [d] Unit cell in full-body/rigid-body minimized structure: 7.712/7.713 Å, 8.286/8.289 Å, 10.415/10.412 Å, 75.68/76.65°, 322.45/322.44 Å^3.

form A is the thermodynamic polymorph and form B is the kinetic phase. The enantiotropic relationship means that lattice-energy differences as small as 0.3 kcal mol^{-1} (~1.3 kJ mol^{-1}) computed using the COMPASS force field (Cerius[2]) are experimentally verified. This value serves as a benchmark for future work on crystal structures that lie in a shallow potential energy well such as concomitant and/or conformational polymorphs. 2) We have shown that weak but directional C–H···O interactions promote multiple molecules in the asymmetric unit and moreover that a short H···O distance in a particular polymorph relates to a high Z' value of that crystal structure. Z' is 4 in kinetic polymorph B and 1 in thermodynamic polymorph A. 3) The reason for conformational polymorphism in **1** is the presence of several low-energy, interconverting conformations in solution. The crystal structures of **1** are a compromise between the minimization of intramolecular (rotamer) and intermolecular (interaction) energies. Crystal packing stabilizes the metastable molecular conformation of **1** in the solid state. 4) Thermodynamic polymorph A is reproduced as frame #3 in full-body minimized structure prediction based on U_{latt}. Re-ranking of frames by including the E_{conf} contribution to the crystal energy gives global minimum structure #1 which matches form A. This exercise gives a posteriori validity to Cerius[2] Polymorph Predictor for a conformationally flexible medium-sized organic molecule. Our results on prototype system **1** are currently being examined and evaluated in other polymorphic clusters.

Experimental Section

Synthesis: Compound **1** was prepared in four steps as shown in Scheme 1.[35]

trans-Stilbene (1.1 g, 6.0 mmol) in CH_2Cl_2 (60 mL) was added dropwise to a stirred solution of *m*-CPBA (1.14 g, 6.6 mmol) in dry CH_2Cl_2 (15 mL) at 0 °C. The reaction was continued for 30 h. The mixture was washed with a $NaHCO_3$ solution and water. The resulting epoxide was extracted with CH_2Cl_2 and evaporated in vacuo to give pure *trans*-stilbene oxide (1.2 g, 95 %).

trans-Stilbene oxide (1.20 g, 6.0 mmol) was stirred with $BF_3{\cdot}Et_2O$ (0.5 mL, 225 mg, 3.0 mmol) in dry CH_2Cl_2 (60 mL) for 30 min at 0 °C. The reaction mixture was washed with water (2 × 50 mL) and the solvent evaporated to give diphenyl acetaldehyde (960 mg, 80 %).

Ethanolic KOH (3 N, 0.5 mL) was added dropwise over a period of 5 min to a mixture of diphenyl acetaldehyde (700 mg, 3.6 mmol) and methyl vinyl ketone (MVK, 0.3 mL, 3.7 mmol) in dry THF (30 mL) at 0 °C. The mixture was stirred for 2 h at 0 °C and then for 2 h at room temperature. Neutralization with 20 % HCl, extraction with EtOAc, and work up gave the crude

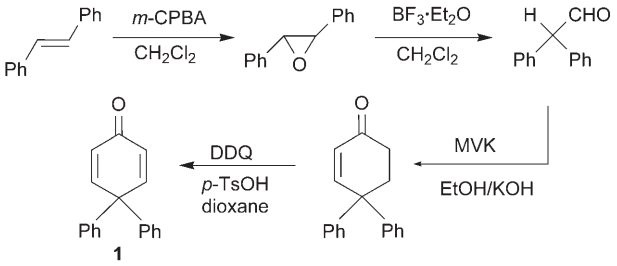

Scheme 1. Synthesis of diphenylquinone **1** from *trans*-stilbene.

product. Purification by column chromatography yielded pure 4,4-diphenyl-2-cyclohexenone (440 mg, 50 %).

DDQ (908 mg, 4.0 mmol) and a catalytic amount of *p*-TsOH (15 mg, 0.1 mmol) was added to a solution of the above cyclohexenone (248 mg, 1.0 mmol) in 1,4-dioxane (40 mL) and the solution was refluxed for 72 h. After cooling, the reaction mixture was filtered through Celite and the filtrate was diluted with CH_2Cl_2 and washed with 10 % NaOH solution (3 × 30 mL). Workup gave the crude product which was purified on a silica gel column to give pure 4,4-diphenyl-2,5-cyclohexadienone **1** (100 mg, 40 %). M.p. 120 °C. ^{1}H NMR (400 MHz, $CDCl_3$, 25 °C, TMS): $\delta = 6.38$ (d, $J = 10$ Hz, 2H, α-enone Hs), 7.25–8.15 (m, 12H, Ph + β-enone Hs) ppm; IR (KBr): $\tilde{\nu} = 3028$, 1655 (C=O), 1620, 1487, 1446, 1400, 1267, 1226 cm^{-1}.

Polymorphs A—D: The pure solid **1** after column chromatography was analyzed by powder XRD. The bulk material (100 mg of the solid) shows all four forms A–D in the concomitant crystallization batch (Figure 3): monoclinic form A 37.5 %, triclinic forms B + C 52.0 %; orthorhombic form D 10.5 %.

Polymorphic forms A, B, and C were crystallized by slow evaporation of a solution of **1** in 5 % EtOAc/*n*-hexane at ambient temperature. Three types of morphologies were observed: needle, block, and plate. Needle-type crystals correspond to form A and block/plate crystals correspond to form B as confirmed by random cell-checking of different crystals. Crystallization by slow evaporation at −5 °C in a domestic refrigerator yielded form A whereas crystal growth from a saturated solution by fast evaporation at ambient temperature yielded predominantly form B. Crystals of form D were obtained from a CH_2Cl_2/EtOAc/*n*-hexane solvent mixture. In recent batches over the last 2–3 years we have not found a single crystal corresponding to form C in several random cell-checking experiments.

Pure form A: The polymorphic mixture **1** (100 mg) was heated in a test tube at ~70 °C in an oil bath for 30 min and then slowly cooled to room temperature. The mixture converted to form A in > 95 % purity as confirmed by powder XRD (Figure 5).

Pure form B: The polymorphic mixture **1** (100 mg) was heated in the aluminium pan of a powder X-ray diffractometer until the compound melted (~120 °C). The cooled solid is form B (powder XRD in Figure 6), as confirmed by unit-cell matching of a few randomly picked crystals.

Differential scanning calorimetry: DSC was performed with a Mettler Toledo 822e module. Samples (4–6 mg) were placed in crimped but vented aluminium pans and heated at 10 °C min^{-1} from 30–200 °C. The instrument was purged with a stream of dry nitrogen at 150 mL min^{-1}.

Spartan 04, Gaussian 03, and Cerius^2 computations: Cerius^2 *simulations and crystal energy*:[26] All simulations were carried out using version 4.8 of the Cerius^2 molecular modeling software package on a Silicon Graphics workstation. Geometry optimization was carried out using density functional theory (DFT) at the B3LYP/6-31G (d,p) level of theory with Gaussian 03.[32] The global minimized rotamer of **1** from Gaussian 03 was entered as the input for the Polymorph Predictor. Crystal structure prediction was carried out in six common space groups ($P2_1$, $P2_1/c$, $C2/c$, $Pbca$, $P2_12_12_1$, and $P\bar{1}$). The cell parameters of predicted frames of the $C2/c$ space group were compared with reduced cell parameters to confirm that they represent different structures. Reduced cell parameters are used throughout the paper. Atom point charges were assigned using the COMPASS force field. It was not felt necessary to calculate multipole charges because molecule **1** does not contain strong hydrogen-bonding groups. Multipole charges are known to give superior results but the advantage is more evident in strongly hydrogen-bonded structures and that too at the expense of an approximate 10-fold increase in computer time.[36] Default options were used throughout with the fine search option in Monte Carlo simulations and for the clustering of frames to obtain unique structures. Lattice-energy minimization of predicted structures was carried out without any modifications except for the use of the Ewald summation of van der Waals interactions at a cut off of 6.0 Å. All calculations were carried out either by relaxing the molecular conformation during the minimization, referred to as the full-body method, or by keeping the conformation fixed during minimization, the so-called rigid-body method. Full-body lattice energy minimizations were carried out even though these calculations take approximately five times more computer time because this method gives more accurate results for flexible molecules such as **1**. The lattice energies of the experimental polymorphs of **1** were computed using the Cerius^2 program by energy minimization of crystal structures using DREIDING 2.21 and COMPASS force fields. Force-field charges were assigned with COMPASS and the charge equilibrium method was used with DREIDING 2.21. COMPASS is better parametrized for structure prediction and the energy of organic molecules. Crystal lattice energies were calibrated to account for the number of molecules in the unit cell (per molecule).

Spartan 04 computations: The energies of all 19 conformers were calculated using Spartan 04[25] with crystallographic coordinates as the input; the positions of the hydrogen atoms were reoptimized at the HF/6-31G** level of theory while keeping the heavy atoms fixed. The gas-phase conformation of **1** was obtained by global energy minimization. The gas-phase rotamer of **1** calculated using Spartan 04 ($\tau_1=\tau_2=22.3°$) is very similar to the minimized conformation derived using Gaussian 03 ($\tau_1=\tau_2=23.8°$).

Variable-temperature powder X-ray diffraction: Powder X-ray data were collected with a PANlytical X'Pert PRO powder X-ray diffractometer using a parallel beam of monochromated Cu-K_α radiation ($\lambda=1.54056$ Å) and an X'celerator detector at 40 kV and 40 mA. Diffraction patterns were collected over the 2θ range of 5–50°. Samples were ground to a particle size of >20 μm and loaded in an 18 mm alumina holder for variable-temperature powder X-ray diffraction data collection and in an aluminium sample holder with a 10 mm diameter sample cavity for the collection of data at room temperature. Vigorous grinding was avoided to minimize potential phase transitions. The program X'Pert High Score was used for the processing and comparison of powder patterns. Powder Cell 2.3[22] was used for calculating the PXRD patterns and for the profile fitting and Rietveld refinement of unit-cell parameters, a displacement parameter, a background polynomial function, peak shape asymmetry terms, and an overall temperature factor using the known single-crystal structures of polymorphs A, B, and D as the model. Variable-temperature powder X-ray diffraction data at a heating rate of 1 °C min^{-1} were collected at $T=28$, 39, 49, 59, 69, 79, 89, 94, 98, 102, and 105 °C. The sample was cooled to room temperature (31 °C) and data were recollected. Powder XRD profiles are plotted in the range of $2\theta=10$–35° for all samples. There are no significant peaks below 10° and only minor peaks between 35 and 50°. Wide peaks resulting from the sample holder appear at 25.2 and 34.8°.

Acknowledgements

We thank the Department of Science and Technology for research funding (SR/S5/OC-02/2002), for support of the CCD X-ray diffractometer (IRPHA), and the CMSD computational facility. The UPE program of the UGC provided infrastructure funds for UH. S.R. and R.B. thank the UGC for fellowships. G.J.K. and Prof. Gautam R. Desiraju (UH) thank the Indo-South Africa Program on Research Cooperation for financial support (DST/INT/SAFR/COP/2001).

[1] W. C. McCrone in *Physics and Chemistry of the Organic Solid State, Vol. 2* (Eds.: D. Fox, M. M. Labes, A. Weissberger), Wiley Interscience, New York, **1965**, pp. 725–767.

[2] J. Bernstein, *Polymorphism in Molecular Crystals*, Clarendon Press, Oxford, **2002**.

[3] For some recent papers on polymorphism dealing with these issues, see: a) A. Kálmán, L. Fábián, G. Argay, G. BernPth, Z. Gyarmati, *J. Am. Chem. Soc.* **2003**, *125*, 34; b) I. Weissbuch, V. Y. Torbeev, L. Leiserowitz, M. Lahav, *Angew. Chem.* **2005**, *117*, 3290; *Angew. Chem. Int. Ed.* **2005**, *44*, 3226; c) M. Morimoto, S. Kobatake, M. Irie, *Chem. Eur. J.* **2003**, *9*, 621; d) P. Raiteri, R. Martoòák, M. Parrinello, *Angew. Chem.* **2005**, *117*, 3835; *Angew. Chem. Int. Ed.* **2005**, *44*, 3769; e) P. K. Thallapally, R. K. R. Jetti, A. K. Katz, H. L. Carrell, K. Singh, K. Lahiri, S. Kotha, R. Boese, G. R. Desiraju, *Angew. Chem.* **2004**, *116*, 1169; *Angew. Chem. Int. Ed.* **2004**, *43*, 1149; f) H. Chow, P. A. W. Dean, D. C. Craig, N. T. Lucas, M. L. Scudder, I. G. Dance, *New J. Chem.* **2003**, *27*, 704; g) R. G. Gonnade, M. M. Bhadbhade, M. S. Shashidhar, *Chem. Commun.* **2004**, 2530; h) C. Guo, M. B. Hickey, E. R. Guggenheim, V. Enkelmann, B. M. Foxman, *Chem. Commun.* **2005**, 2220; i) S. Aitipamula, A. Nangia, *Chem. Commun.* **2005**, 3159; j) W. I. F. David, K. Shankland, C. R. Pulham, N. Bladgen, R. J. Davey, M. Song, *Angew. Chem.* **2005**, *117*, 7194; *Angew. Chem. Int. Ed.* **2005**, *44*, 7032.

[4] G. R. Desiraju, *Angew. Chem.* **1995**, *107*, 2541; *Angew. Chem. Int. Ed. Engl.* **1995**, *34*, 2311.

[5] a) R. J. Davey, *Chem. Commun.* **2003**, 1463; b) N. Blagden, R. J. Davey, *Cryst. Growth Des.* **2003**, *3*, 873; c) P. Erk, H. Hengelsberg, M. F. Haddow, R. van Gelder, *CrystEngComm* **2004**, *6*, 474; d) J. Bernstein, *Chem. Commun.* **2005**, 5007; e) L. Yu, *J. Am. Chem. Soc.* **2003**, *125*, 6380; f) P. Vishweshwar, J. A. McMahon, M. Oliveira, M. L. Peterson, M. J. Zaworotko, *J. Am. Chem. Soc.* **2005**, *127*, 16802; g) C. P. Price, A. L. Grzesiak, A. J. Matzger, *J. Am. Chem. Soc.* **2005**, *127*, 5512.

[6] S. R. Bryn, R. R. Pfeiffer, J. G. Stowell, *Solid-State Chemistry of Drugs*, SSCI, West Lafayette IN, **1999**.

[7] a) X. Zheng, B. Wang, U. Engelert, G. E. Herberich, *Inorg. Chem.* **2001**, *40*, 3117; b) J. van de Streek, S. Motherwell, *Acta Crystallogr. Sect. B* **2005**, *61*, 504. In 2000 the values were 4.1% of organic compounds and 5.5% of organometallic compounds (ref. [7a]), which in 2004 was updated to 14600 accurate crystal structures out of 325000 entries (4.5%) (ref. [7a]).

[8] F. H. Allen, R. Taylor, *Chem. Soc. Rev.* **2004**, *33*, 463. The CSD is an archive of over 350000 small-molecule organic and organometallic crystal structures (August 2005 release); see www.ccdc.cam.ac.uk

[9] a) L. Yu, G. A. Stephenson, C. A. Mitchell, C. A. Bunnell, S. V. Snorek, J. J. Bowyer, T. B. Borchardt, J. G. Stowell, S. R. Byrn, *J. Am. Chem. Soc.* **2000**, *122*, 585; b) S. Chen, I. A. Guzei, L. Yu, *J. Am. Chem. Soc.* **2005**, *127*, 9881.

[10] a) V. S. S. Kumar, PhD Thesis, University of Hyderabad, **2002**; b) crystal structures of **3** have been deposited with the Cambridge Crystallographic Data Centre (see ref. [8]): CCDC 293133–293135.
[11] J. Bernstein, R. J. Davey, J.-O. Henck, *Angew. Chem.* **1999**, *111*, 3646; *Angew. Chem. Int. Ed.* **1999**, *38*, 3440.
[12] J. Bernstein in *Organic Solid State Chemistry* (Ed.: G. R. Desiraju), Elsevier, Amsterdam, **1987**, pp. 471–518.
[13] a) V. S. S. Kumar, A. Addlagatta, A. Nangia, W. T. Robinson, C. K. Broder, R. Mondal, I. R. Evans, J. A. K. Howard, F. H. Allen, *Angew. Chem.* **2002**, *114*, 4004; *Angew. Chem. Int. Ed.* **2002**, *41*, 3848; b) A. Nangia in *Nanoporous Materials: Science and Engineering* (Eds.: G. Q. Lu, X. S. Zhao), Imperial College Press, London, **2004**, pp. 165–187.
[14] G. R. Desiraju, *Acc. Chem. Res.* **2002**, *35*, 565.
[15] J. Bernstein, R. E. Davis, L. Shimoni, N.-L. Chang, *Angew. Chem.* **1995**, *107*, 1687; *Angew. Chem. Int. Ed. Engl.* **1995**, *34*, 1555.
[16] V. S. S. Kumar, A. Nangia, *Chem. Commun.* **2001**, 2392.
[17] J. W. Steed, *CrystEngComm* **2003**, *5*, 169.
[18] a) C. P. Brock, L. L. Duncan, *Chem. Mater.* **1994**, *6*, 1307; b) C. P. Brock, *Acta Crystallogr. Sect. B* **2002**, *58*, 1025.
[19] A. Gavezzotti, G. Fillippini, *J. Phys. Chem.* **1994**, *98*, 4831.
[20] H. Jacobsen, H. W. Schmalle, A. Messmer, H. Berke, *Inorg. Chim. Acta* **2000**, *306*, 153.
[21] K. E. Plass, K. Kim, A. J. Matzger, *J. Am. Chem. Soc.* **2004**, *126*, 9042.
[22] Rietveld refinement was carried out using Powder Cell 2.3, N. Krauss, G. Nolze, Federal Institute for Materials Research and Testing, Berlin, **2000**.
[23] a) J. D. Dunitz, J. Bernstein, *Acc. Chem. Res.* **1995**, *28*, 193; b) J.-O. Henck, J. Bernstein, A. Ellern, R. Boese, *J. Am. Chem. Soc.* **2001**, *123*, 1834.
[24] W. Ostwald, *Z. Phys. Chem.* **1897**, *22*, 289. Ostwald's rule of stages: "When leaving a metastable state, a given chemical system does not seek out the most stable state, rather the nearest metastable one that can be reached with minimum loss of free energy."
[25] Spartan 04 computational methods include Hartree–Fock, density function theory, and Moøller–Plesset on an interactive PC interface: see www.wavefun.com
[26] Crystal Packer and Polymorph Predictor of the Cerius^2 suite of software were used for crystal lattice energy calculation and crystal structure prediction: see www.accelrys.com
[27] A. Dey, M. T. Kirchner, V. R. Vangala, G. R. Desiraju, R. Mondal, J. A. K. Howard, *J. Am. Chem. Soc.* **2005**, *127*, 10545.
[28] H. Sun, *J. Phys. Chem.* B **1998**, *102*, 7338.
[29] a) T. C. Lewis, D. A. Tocher, S. L. Price, *Cryst. Growth Des.* **2004**, *4*, 979; b) C. Ouvard, S. L. Price, *Cryst. Growth Des.* **2004**, *4*, 1119; c) H. Nowell, S. L. Price, *Acta Crystallogr. Sect. B* **2005**, *61*, 558.
[30] a) J. D. Dunitz, A. Gavezzotti, *Cryst. Growth Des.* **2005**, *5*, 2180. The ΔE_{total} maximum is larger in ROY (5 kcal mol^{-1} between the Y and ORP forms) because E_{conf} and U_{latt} contributions are additive than in **1** (< 1 kcal mol^{-1}) when the components counter one another.
[31] a) W. D. S. Motherwell, H. L. Ammon, J. D. Dunitz, A. Dzyabchenko, P. Erk, A. Gavezzotti, D. W. M. Hofmann, F. J. J. Leusen, J. P. M. Lommerse, W. T. M. Mooij, S. L. Price, H. Scheraga, B. Schweizer, M. U. Schmidt, B. P. van Eijck, P. Verwer, D. E. Williams, *Acta Crystallogr. Sect. B* **2002**, *58*, 647; b) G. M. Day, W. D. S. Motherwell, H. Ammon, S. X. M. Boerrigter, R. G. Della Valle, E. Venuta, A. Dzyabchenko, J. D. Dunitz, B. Schweizer, B. P. van Eijck, P. Erk, J. C. Facelli, V. E. Bazterra, M. B. Ferraro, D. W. M. Hofmann, F. J. J. Leusen, C. Liang, C. C. Pantelides, P. G. Karamertzanis, S. L. Price, T. C. Lewis, H. Nowell, A. Torrisi, H. A. Scheraga, Y. A. Arnautova, M. U. Schmidt, P. Verwer, *Acta Crystallogr. Sect. B* **2005**, *61*, 511.
[32] Gaussian 03 (Revision B.05), M. J. Frisch, G. W. Trucks, H. B. Schlegel, G. E. Scuseria, M. A. Robb, J. R. Cheeseman, J. A. Montgomery, Jr., T. Vreven, K. N. Kudin, J. C. Burant, J. M. Millam, S. S. Iyengar, J. Tomasi, V. Barone, B. Mennucci, M. Cossi, G. Scalmani, N. Rega, G. A. Petersson, H. Nakatsuji, M. Hada, M. Ehara, K. Toyota, R. Fukuda, J. Hasegawa, M. Ishida, T. Nakajima, Y. Honda, O. Kitao, H. Nakai, M. Klene, X. Li, J. E. Knox, H. P. Hratchian, J. B. Cross, C. Adamo, J. Jaramillo, R. Gomperts, R. E. Stratmann, O. Yazyev, A. J. Austin, R. Cammi, C. Pomelli, J. W. Ochterski, P. Y. Ayala, K. Morokuma, G. A. Voth, P. Salvador, J. J. Dannenberg, V. G. Zakrzewski, S. Dapprich, A. D. Daniels, M. C. Strain, O. Farkas, D. K. Malick, A. D. Rabuck, K. Raghavachari, J. B. Foresman, J. V. Ortiz, Q. Cui, A. G. Baboul, S. Clifford, J. Cioslowski, B. B. Stefanov, G. Liu, A. Liashenko, P. Piskorz, I. Komaromi, R. L. Martin, D. J. Fox, T. Keith, M. A. Al-Laham, C. Y. Peng, A. Nanayakkara, M. Challacombe, P. M. W. Gill, B. Johnson, W. Chen, M. W. Wong, C. Gonzalez, J. A. Pople, Gaussian, Inc., Pittsburgh, PA, **2003**.
[33] The value of U_{latt} for minimized crystal structures after full-body minimization is much lower (ca. −92 kcal mol^{-1}) than rigid-body minimized structures (ca. −32 kcal mol^{-1}). The contribution from valence terms (bonds, angles, torsions, cross-terms) is around −60 kcal mol^{-1} for full-body minimization of molecule **1** but valence terms are not considered in rigid-body minimization (fixed to zero). This difference between the two sets of energies is not a problem because we are comparing relative energies using the same method.
[34] For CSP and isolation of the polymorph, see: a) A. T. Hulme, S. L. Price, D. A. Tocher, *J. Am. Chem. Soc.* **2005**, *127*, 1116; b) G. M. Day, A. V. Trask, W. D. S. Motherwell, W. Jones, *Chem. Commun.* **2006**, 54.
[35] a) D. J. Reif, H. O. House, *Org. Syn.* **1963**, *Coll. Vol. IV*, 860; b) D. J. Reif, H. O. House, *Org. Syn.* **1963**, *Coll. Vol. IV*, 375; c) A. C. Cope, P. A. Trumbell, E. R. Trumbell, *J. Am. Chem. Soc.* **1958**, *80*, 2844; d) H. E. Zimmerman, K. G. Hancock, G. C. Licke, *J. Am. Chem. Soc.* **1968**, *90*, 4892; e) K.-B. Chai, P. Sampson, *J. Org. Chem.* **1993**, *58*, 6807.
[36] G. M. Day, W. D. S. Motherwell, W. Jones, *Cryst. Growth Des.* **2005**, *5*, 1023.

Received: November 15, 2005
Published online: March 3, 2006

